

Experimental Study of Torque Measurement Based On FBG

Shengnan Fu, Yinguo Huang, and Xinghua Li

Abstract This paper discusses a method of torque measurement based on the fiber Bragg grating (FBG) sensor, and introduces the FBG's application for torque measurement in a rotating shaft with four same planes. With external torsion applied to the shaft, the data obtained by finite element analysis verified the rationality, reliability and strain sensitivity of this design. One end of the shaft is fixed, while the other is connected to a device providing a particular value of torsion with a full scale of 100 Nm. Two parallel gratings FBG1 and FBG2 are bonded on the purposefully machined planes on the shaft symmetrically. Considering the differential-mode wavelength of the dual-grating torsion sensor, the result shows a low temperature sensitivity and a high torsion sensitivity. The sensitivity of the torque measurement system is 14.5 pm/Nm, and has a high linearity and linear correlation.

Keywords Torque measurement • Fiber Bragg grating • Finite element analysis • Optical fiber sensors

1 Introduction

Torque sensing is very important in industrial production and is widely needed in the field of ship and aviation, aerospace especially in special applications in harsh environments where torque measurement is often presented as technical bottlenecks. Optical fiber sensors are paid great attention because of many desirable properties such as immunity to electromagnetic interference, their multiplexing capability and small size [1]. Tian X.M. et al. proposed a fiber sensor using a single fiber Bragg grating that is bonded to a shaft at the appropriate angle [2]. As the

S. Fu (✉) • Y. Huang • X. Li

State Key Laboratory of Precision Measuring Technology and Instruments, Tianjin University,

Tianjin 300072, China

e-mail: fsn666@163.com

deviation caused by temperature cannot be eliminated, the accuracy of the fiber sensor remains to be improved. In 2003, Zhang W.G. in Nankai University designed a linear torsion sensor with very little temperature dependence, the torque sensor sensitivity is as high as 2.076 nm/Nm, with torsion angle changing in $\pm 40^\circ$ [3]. But the device is not suited to any application especially in the industry because of its unusual structure and the weak mechanical strength of the organic material shaft. Kruger et al. researched that a fiber sensor comprised of two cascaded Bragg gratings with distinct resonance wavelengths showed if the FBGs are mounted at angles of $+45^\circ$ and -45° with respect to the longitudinal axis of the shaft, the differential-mode wavelength will be proportional to torsion with very little temperature dependence [4].

2 Background Theory

According to fiber grating coupled mode theory, central wavelength of reflectance spectrum satisfy the following conditions: $\lambda_B = 2n_{eff}\Lambda$ [5], where λ_B is Bragg central wavelength, n_{eff} is the effective index of refraction of the core mode, Λ is the period of the grating. It is apparent that central wavelength will change following the change of n_{eff} and Λ , which leads shift of FBG center wavelength $\Delta\lambda_B$ is function of strain ε and temperature T . So the equation can be written as:

$$\begin{aligned} \frac{\Delta\lambda_B}{\lambda_B} &= \left[\frac{1}{n_{eff}} \frac{\partial n_{eff}}{\partial \varepsilon} + \frac{1}{\Lambda} \frac{\partial \Lambda}{\partial \varepsilon} \right] \Delta\varepsilon + \left[\frac{1}{n_{eff}} \frac{\partial n_{eff}}{\partial T} + \frac{1}{\Lambda} \frac{\partial \Lambda}{\partial T} \right] \Delta T \\ &= (\alpha_f + \xi) \Delta T + (1 - p_e) \Delta\varepsilon \end{aligned} \quad (1)$$

where α_f is the coefficient of thermal expansion of the fiber, representing the period of the grating varies with temperature; ξ is the thermo-optical coefficient of fiber material, representing the index of refraction varies with temperature and p_e is the elasto-optical coefficient of fiber material, representing the refractive index varies with strain.

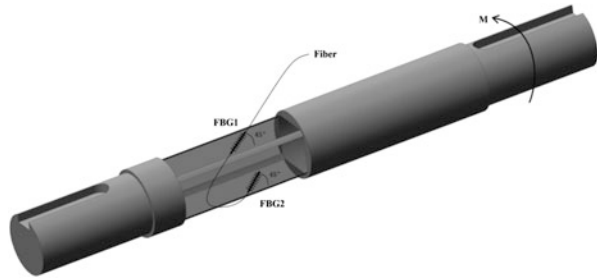
When a static torque applied to the shaft having a radius of r , the elastic deformation should produces a shear strain, assuming that the deformation is too small to alter the length and cross-section of the shaft. The total shear is given by:

$$M = \frac{\tau \cdot G \cdot I}{r} \quad (2)$$

where M is the torsion, τ is the shear, G is the shear modulus of the material and I is the polar moment of inertia of the shaft.

As shown in Fig. 1, the shaft, with its length $L = 180$ mm and radius $r = 20$ mm, is shaved into four planes between the axis of the cylindrical portion in the middle to bond fiber grating and increase the axis's sensitivity. Supposing the FBGs are

Fig. 1 The design of the shaft and situation of FBGs bonded on the planes



mounted on the two symmetrical planes at angles α and $-\alpha$ with respect to the cross section of the shaft, FBG's strain is given by:

$$\Delta\epsilon_s = \frac{r \sin 2\alpha}{2GI} M \quad (3)$$

It is well known that the gratings will experience principal strains of the same magnitude but opposite in sign, if the shaft is subjected to pure torsion. As following equation shows:

$$\begin{cases} \Delta\lambda_1 = (1-p_e)\lambda_1 \\ \Delta\lambda_2 = -(1-p_e)\lambda_2 \end{cases} \quad (4)$$

$\Delta\lambda_1$, $\Delta\lambda_2$ are the changes in the resonant wavelengths of the gratings FBG1 and FBG2 respectively. We define the differential-mode wavelengths of these two gratings as follows:

$$\Delta\lambda = \Delta\lambda_1 - \Delta\lambda_2 = (1-p_e) \cdot \Delta\epsilon_s \cdot (\lambda_1 + \lambda_2) \quad (5)$$

As gratings' common-mode wavelengths $\lambda_{cm} = \frac{1}{2}(\lambda_1 + \lambda_2)$ always remain unchanged, the strain sensitivity of the gratings is given by: $K_\epsilon = 1 - p_e$. The relationship between the change of central wavelength $\Delta\lambda$ and the torque M can be described as:

$$\Delta\lambda = \frac{\lambda_m \cdot K_\epsilon \cdot r \sin 2\alpha}{GI} \cdot M \quad (6)$$

Differential-mode wavelength of the FBGs remains for the most part unaffected by temperature [6], we can use this method to obtain the desired precision in torque measurement.

3 Finite Element Analysis and Simulation

Finite element analysis can shorten the cycle of design and analysis, make a better solution of product design, reduce the material consumption or cost, and discover potential problems of product manufacture or engineering construction in advance. The virtual prototype effect of CAE design has largely replaced physical prototype based design and verification process with huge resource consumption in conventional design. It can predict the product reliability throughout the whole lifecycle, and ensure the rationality of product design.

Firstly, the material of the shaft is defined as solid187 element with 10-nodes tetrahedral structure, which can simulate the situation of bending moment and torque. The element also has plasticity, hyper elasticity, creep, stress stiffening, large deflection, and large strain capabilities. Create a single node on the centerline out of the shaft, and define it as mass21 element, which is structural mass with six degrees of freedom. A different mass and rotary inertia may be assigned to each coordinate direction. The element coordinate system hardly rotates with the nodal coordinate rotations during a small deflection analysis. And due to small deflection of the shaft in this experiment, the 3-D mass will obtain moment of inertia by setting $KEYOPT(3) = 0$, which leads to six degrees of freedom of the node.

Secondly, import geometric model of the shaft to the ANSYS software, and the meshing will be applied to this geometry. A rigid connection is coupled between the major node and all the nodes of end face via “cerig” order. Due to the transitivity of torque, the torque will pass to the entire shaft, when loaded on the major node, which can also avoid the phenomenon of stress concentration caused by the torque loaded directly on the end face.

Finally, Constraints and loads are applied to the shaft, and the result will be displayed by the solver. The software will give the data of strain, deformation, shear force and stress distribution diagrams of the shaft under a torque of 100 Nm, from which the value computed by finite element analysis is to be compared with material mechanical properties to judge whether the material meets the requirements and whether the design is rational.

The material selected in this experiment is quenched and tempered steel of 40CR. Its shear modulus $G = 80.8$ GPa, Poisson's ratio $\mu = 0.31$, the yield limit is 800 MPa, the allowable stress is 400 MPa, and the allowable stress in shear is 280 MPa. The distribution diagrams of deformation, shear stress, and equivalent stress intensity for a torque of 100 Nm is showed in Fig. 2. All the values computed are in acceptable range of material, meeting the requirements absolutely. Strain distribution of the shaft as shown in Fig. 3, indicates that the planes have a better strain sensitivity than other parts of the shaft.

Sensor sensitivity is related to the length, both inside and outside diameter and material properties of the shaft, so it's feasible to obtain a higher sensitivity by optimizing the shaft's relevant parameters. The determination of the measuring range (including temperature variation range) should follow the principle of avoiding destroying the fiber gratings and ability to keep shaft's elasticity.

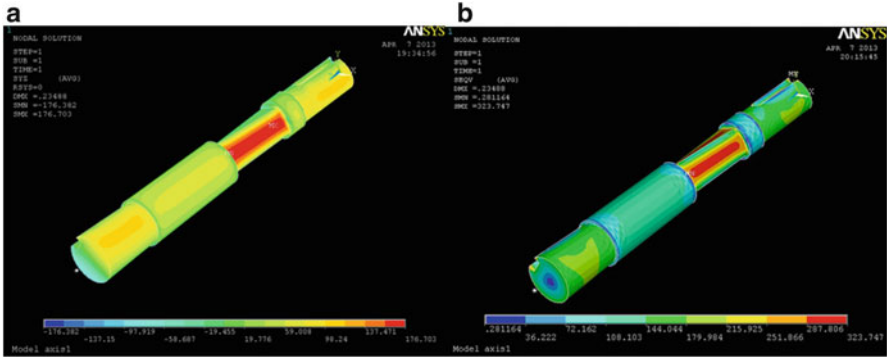


Fig. 2 Simulation result. (a) Shear stress distribution of the shaft in SYZ direction, (b) equivalent stress distribution of the shaft based on the fourth strength theory

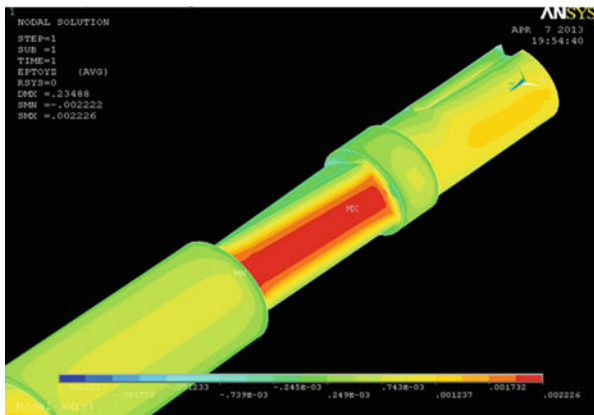


Fig. 3 Strain distribution of the plane

4 Experiment and Results

Experimental apparatus is composed of fixed platform, torque loading device, shaft, FBG interrogator and the host computer. Torque loading device can provide a particular value of torque with a full scale of 100 Nm; the real-time data processing, display and other correlation manipulations are run by the host computer, which is connected to the FBG interrogator through the TCP/IP port.

The torque is applied to one end of the shaft, while the other is fixed. And then strain can be reflected by the FBG sensors. According to the photosensitivity of FBG, we can obtain the wavelength shift by the FBG interrogator, and thus calculate the torque value of the shaft.

Experimental data and its fitting curve of FBG1 and FBG2 are showed in Fig. 4 respectively. As for FBG1, the determination coefficient is equal to $R^2 = 0.9997$,

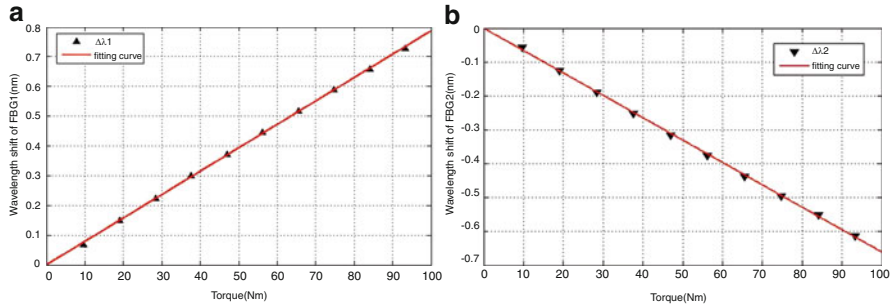


Fig. 4 Experimental data of FBG1 and FBG2. (a) Wavelength shift of FBG1 as a function of torque, (b) wavelength shift of FBG1 as a function of torque

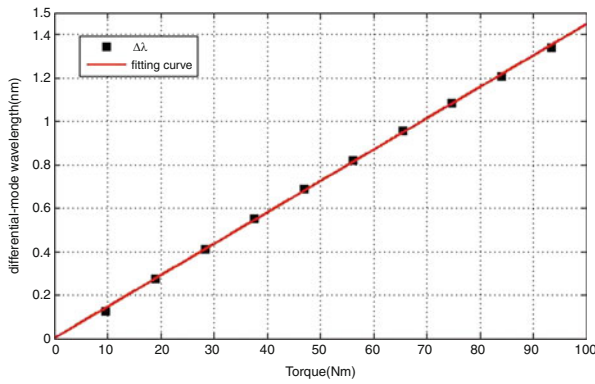


Fig. 5 Differential-mode wavelength of the two FBGs as a function of torque

the square sum of error $SSE = 0.000154$ and the root mean square error $RMSE = 0.004388$, while for FBG2 $R^2 = 0.9994$, $SSE = 0.0001776$, $RMSE = 0.004712$. The result indicates that FBG in tensile state has a more ideal linearity than that in compression state.

The relationship between the change of differential-mode wavelength as a function of torque and its fitting curve are shown in Fig. 5, with key indexes of $R^2 = 0.9996$, $SSE = 0.0006519$, $RMSE = 0.009027$. Although linearity compared with FBG1 falls slightly, the sensitivity is double, with value of 14.5 pm/Nm and linear correlation coefficient is 0.99978, suggesting that the accuracy of this structure is relatively good.

5 Conclusion

Torque measurement technology based on fiber gratings has incomparable advantages for many desirable characteristics of fiber grating, such as insulation, anti-electromagnetic interference. This paper analyzes a method using two fiber gratings to measure torque with lower temperature affect. The shaft is elaborately designed in purpose of mounting fiber gratings in a more user-friendly way and optimizing its sensitivity. By finite element analysis we have verified its safety, rationality, stability of the mechanical structure, and got further understanding of the relevant characteristics of the shaft. The experimental apparatus has a torque sensitivity with value of 14.5 pm/Nm and high linearity, having laid the theoretical and experimental basis for large torque measurement and distributed measurement in the future.

References

1. Kersey AD, Davis MA, Patrick HJ, LeBlanc M, Koo KP, Askins CG, Putnam MA, Friebele EJ (1997) Fiber grating sensors: fiber gratings, photosensitivity, and poling. *J Lightwave Technol* 15(8):1442–1463
2. Tian XG, Tao XM (2000) Torsion measurement by using FBG sensors. *Proc SPIE* 4077:154–164
3. Zhang WG, Kai GY, Dong X, Yuan S, Zhao Q (2002) Temperature-independent FBG-type torsion sensor based on combinatorial torsion beam. *Photon Technol Lett IEEE* 14(8):1154–1156
4. Kruger L, Swart PL, Chtcherbakov AA, van Wyk AJ (2004) Non-contact torsion sensor using fibre Bragg gratings. *Meas Sci Technol* 15(8):1448–1452
5. Othonos A, Kalli K (1999) *Fiber Bragg gratings: fundamentals and applications in telecommunications and sensing*. Artech House, Boston
6. Swart PL, Chtcherbakov AA, van Wyk AJ (2005) Bragg grating sensor for torsion and temperature measurements in rotating machinery. *Proc SPIE* 5634:353–360